Numerical Simulation of Pulverised Coal Combustion

V. Sahajwalla[1], A. Eghlimi[2] and K. Farrell[1]

1. School of Material Science and Engineering
2. Center for Advanced Numerical Computation in Engineering and Science (CANCES)
The University of New South Wales, Sydney 2052, Australia

ABSTRACT

Pulverised coal combustion in a 2D furnace has been numerically studied. Two methods have been employed to simulate combustion modelling. The first method is a generalised finite rate formulation, known as the Magnussen model, which is based on the solution of species transport equation for reactants and product concentrations. The second method known as the mixture fraction PDF/formulation solves a single conserved scalar (the mixture fraction) transport equation. The reaction rate that appear as source terms in the species transport equations are computed from either Arrhenius rate expressions or the two competing rates of Kobayashi (1976) model. The coal type K of the study accomplished by Smith *et al.* (1989) has been chosen for the present simulation. The results show the advantages of the PDF model versus the finite rate model, but more importantly it illustrates the role of CFD in detailed analysis of a furnace.

1. INTRODUCTION

Pulverised coal combustion is one of the major sources in producing energy for power plants. It also provides a significant amount of pollutants. Therefore, understanding the combustion process will improve the efficiency of power plants and reduce the air pollution. Combustion is a complicated process which consists of a poly-dispersed mixture of reactant, combustion product gases and solid particles consisting of coal, char, fly-ash and soot.

Therssen, *et al.* (1995), investigated experimentally and numerically the devolatilisation of high volatile bituminous coal particles under a rapid heating conditions. Five models of devolatilisation were tested and compared with the experimental results. They obtained acceptable results for flame's peak temperature. Goerres *et al.* (1995) in the study of trajectory of burning coal investigated the mass loss of the coal particles due to devolatilisation and char burnout. The influence of the gas-phase turbulence modelling on the particle motion were also studied In the present research, the combustion simulation with the generalised finite rate chemistry model, referred to as the Magnussen model and the reacting flow with the mixture fraction PDF/equilibrium chemistry model, referred to as the PDF model are studied.

2. NUMERICAL PROCEDURE

A generalised finite volume based CFD code, FLUENT, was utilised for modelling the pulverised coal combustion. In addition to solving transport equations for continuity, momentum, energy, turbulence kinetic energy, dissipation and species, the dispersed second phase is simulated in a Lagrangian frame of reference. The coal particles are taken to be spherical.

In a Lagrangian reference frame the trajectory of the particles is calculated by integrating the force balance on the particle which can be written as follows in Cartesian coordinates:

$$\frac{du_p}{dt} = F_D(u - u_p) + \frac{g\,(\rho_s - \rho)}{\rho_s} + F_x \qquad (1)$$

where $F_D(u-u_p)$ is the drag force per unit particle mass and is defined based on particle Reynolds number as follows:

$$F_D = \frac{18\mu}{\rho_s D_p^2}\frac{C_D \mathrm{Re}_p}{24} \qquad (2)$$

In Equations (1) and (2), u is the gas velocity, u_p is the particle velocity, μ is the molecular viscosity of the gas, ρ is the fluid density, ρ_s is the particulate density and D_p is the particle diameter. Re_p is the particulate Reynolds number:

$$Re_p = \frac{\rho |u - u_p| D_p}{\mu} \quad (3)$$

The drag coefficient, C_D, in equation (2) is defined as:

$$C_D = \Xi_1 + \Xi_2 \frac{1}{\mathrm{Re}_p} + \Xi_3 \frac{1}{\mathrm{Re}_p^2} \quad (4)$$

where the constants Ξ_1, Ξ_2 and Ξ_3 are given by Morsi and Alexander (1977) based on different ranges of Re. In equation (1) F_x is any additional force such as: 1) Virtual mass force (the force required to accelerate the fluid surrounding the particle) which is important when $\rho > \rho_p$. 2) The force due to the pressure gradient in the fluid. 3) Any additional forces (e.g., electrostatic forces). In the present study $F_x=0$.

Solution of the dispersed phase requires integration in time of the force balance on the particle to yield the particle trajectory. The accuracy of the dispersed phase calculation thus depends on the time accuracy of the integration. The trajectory equations are solved by step-wise integration over discrete time steps. Integration in time of equation (1) yields the velocity of the particle at each point along the trajectory via:

$$\frac{dx_i}{dt} = u_p \quad (5)$$

Equations (1) and (5) are solved in each coordinate direction to predict the trajectories.

3. HEAT AND MASS TRANSFER CALCULATIONS

3.1 Inert heating

While the particle temperature is less than the vaporization temperature and after the volatile fraction of a particle has been consumed the inert heating law is applied:

$$m_p C_p \frac{dT_p}{dt} = hA_p(T_\infty - T_p) + \varepsilon_p A_p \sigma(\theta_R^4 - T_p^4) \quad (6)$$

where, m_p is the mass of the particle (Kg), C_p is the heat capacity of the particle (J/Kg-K), A_p is the surface area of the particle (m^2), T_∞ is the local temperature of the gas phase (K), T_p is the particle temperature, h is the convective heat transfer coefficient (W/m^2-K), ε_p is the particle emissivity, $\sigma=5.67 \times 10^{-8}$ W/m^2K^4 is the Boltzmann's constant and θ_R is the radiative temperature. It has been assumed in Equation (6) that the particle is at a uniform temperature throughout. Equation (6) is integrated in time using an approximate, linearised, form that assumes that the particle temperature changes slowly from one time value to the next:

$$m_p c_p \frac{dT_p}{dt} = A_p\left\{-\left[h + \varepsilon_p \sigma T_p^3\right]T_p + \left[hT_\infty + \varepsilon_p \sigma \theta_R^4\right]\right\} \quad (7)$$

The particle temperature is obtained as the particle trajectory is computed via:

$$T_p(t + \Delta t) = \alpha_p + \left(T_p(t) - \alpha_p\right)\exp\left(-\beta_p \Delta t\right) \quad (8)$$

Where Δt is the integration time step where,

$$\alpha_p = \frac{hT_\infty + \varepsilon_p \sigma \theta_R^4}{h + \varepsilon_p \sigma T_p^3(t)} \quad (9)$$

and

$$\beta_p = \frac{A_p(h + \varepsilon_p \sigma T_p^3(t))}{m_p c_p} \quad (10)$$

The heat transfer coefficient, h, is evaluated using the following correlations:

$$Nu = \frac{hD_p}{k_\infty} = 2.0 + 0.6\mathrm{Re}_D^{1/2}\,\mathrm{Pr}^{1/3} \quad (11)$$

where, k_∞ is the thermal conductivity of the continuous phase (W/mk) and P_r is the Prandtl number of the continuous phase. As the particle traverses each computational cell, the heat lost or gained appears as a source term in the energy equation.

3.2 Coal Devolatilisation

When the temperature of the particle reaches the vaporization temperature, T_{vap}, the devolatilisation law is applied. Two devolatilisation models have been employed in this paper.

The first model (Badzioch and Hawksley, 1970) is known as the single kinetic rate model that assumes the rate of devolatilization is first order dependent on the amount of volatiles remaining in the particle:

$$-\frac{dm_p}{dt} = k(m_p - (1-f_{v0})m_{p0}) \qquad (12)$$

where, m_p is the particle mass (kg), f_{v0} is the fraction of volatiles initially present in the particle, m_{p0} is the initial particle mass (kg) and k is the kinetic rate (s^{-1}) defined by input of an Arrhenius type pre-exponential, A_1, and activation energy

$$k = A_1 \exp(-E/RT) \qquad (13)$$

The values of A_1 and E were obtained from literature (Smith *et al.*, 1989). Assuming that the particle temperature varies only slightly between discrete time integration steps, the approximate analytical solution yields:

$$m_p(t+\Delta t) = (1-f_{v0})m_{p0} + \left[m_p(t) - (1-f_{v0})m_{p0}\right]\exp(-k\Delta t) \qquad (14)$$

The second model (Kobayashi, 1976) provides the kinetic devolatilisation rate expressions of the form:

$$R_1 = A_1 \exp(-E_1/RT_p) \qquad (15)$$

$$R_2 = A_2 \exp(-E_2/RT_p) \qquad (16)$$

where, R_1 and R_2 are competing rates that may control the devolatilisation over different temperature ranges. The two kinetic rates are weighted to yield an expression for the devolatilisation as:

$$\frac{m_v(t)}{m_{p0}-m_a} = \int_0^t (\alpha_1 R_1 + \alpha_2 R_2)\exp(-\int_0^t (R_1+R_2)dt)dt \qquad (17)$$

where, $m_v(t)$ is the volatile yield up to time t, m_{p0} is the initial mass at injection, α_1 and α_2 are yield factors, taken to be 0.3 and 1.0 for the first (slow) reaction and second (fast) reaction respectively and m_a is the ash content. Kobayashi (1976), recommend that α_1 be set to the fraction of volatiles determined by proximate analysis, since this rate represents devolatilisation at low temperature. The second yield factor, α_2, should be set close to unity, which is the yield of volatiles at very high temperature.

Particle diameter changes during devolatilisation significantly. Particle swelling during devolatilisation has been characterized by the swelling coefficient, C_{sw} which is applied in the following relationship:

$$D_p / D_{p0} = 1 + (C_{sw} - 1)\frac{m_{p0} - m_p}{f_{v0} m_{p0}} \qquad (18)$$

where, D_{p0} and D_p are the initial and the current particle diameter respectively. The swelling coefficient is taken to be 2 for the present study, which means that the final particle diameter doubles when all of the volatile component has vaporized.

4. COMBUSTION MODELLING

4.1 Generalised Finite Rate Modelling

Two reaction modelling approaches have been employed in this study. The first approach, generalized finite rate formulation, solves the species transport equations for reactants and product concentrations, in which the chemical reaction mechanism is explicitly defined. The source of chemical species i′ due to reaction, $R_{i'}$, is computed as the sum of the reaction sources over the k reactions that the species may take part in:

$$R_{i'} = \sum_k R_{i',k} \quad (19)$$

where, $R_{i',k}$ is the rate of creation/destruction of species i′ in reaction k. The reaction rate, $R_{i',k}$, has been calculated by the mixing of the turbulent eddies containing fluctuating species concentrations, known as the eddy breakup model (Magnussen and Hjertager, 1976). This model takes into account the influence of turbulence on the reaction rate. In this approach the smallest of the following values is used for the rate of reaction, $R_{i',k}$:

$$R_{i',k} = \nu'_{i',k} M_{i'} A \rho \frac{\varepsilon}{k} \frac{m_R}{\upsilon'_{R,k} M_R} \quad (20)$$

$$R_{i',k} = \nu'_{i',k} M_{i'} A B \rho \frac{\varepsilon}{k} \frac{\Sigma_p m_R}{\Sigma_p \upsilon'_{R,k} M_R} \quad (21)$$

where m_p and m_R are the mass fraction of any product species, P, and a particular reactant, R, respectively. The empirical constants A and B are taken to be 4.0 and 0.5 respectively. $M_{i'}$, is the molecular weight of species i′ (kg/kmol) and $\nu_{i',k}$ represents the exponent on the concentration of reactant i′ in reaction k. This model relates the rate of reaction to the rate of dissipation of the reactant and product containing eddies.

4.2 Mixture Fraction/PDF Modelling

In the second approach, namely, the mixture fraction/PDF modelling, individual species transport equations are not solved. Instead, the solution of a single conserved scalar transport equation, the mixture fraction, is solved. The individual component concentrations are derived from the predicted mixture fraction distribution. This approach offers many benefits over the finite rate formulation approach. In this method turbulence effects are accounted for by employing a probability density function and reaction mechanisms, which are not explicitly defined. The mixture fraction, f, (Sivathann and Faeth, 1990) which is a single conserved scalar is related to the instantaneous thermo-chemical state of the fluid via:

$$f = \frac{Z_k - Z_{kO}}{Z_{kF} - Z_{kO}} \quad (22)$$

where Z_k is the mass fraction for some element k. Subscripts O and F denote the values at the oxidizer stream and fuel stream inlet, respectively. The mixture fraction, f, is a conserved quantity and its value at each control volume is calculated via the solution of the following transport equation for the mean (time –averaged) value of f:

$$\frac{\partial}{\partial t}(\rho \overline{f}) + \frac{\partial}{\partial x_i}(\rho u_i \overline{f}) = \frac{\partial}{\partial x_i}\left(\frac{\mu_t}{\sigma_t}\frac{\partial \overline{f}}{\partial x_i}\right) + S_m \quad (23)$$

The source term, Sm, is due to transfer of mass into the gas from reacting coal particles. In the PDF approach, the variance of mixture fraction, $\overline{f'^2}$, is calculated via the following transport equation:

$$\frac{\partial}{\partial t}\left(\rho \overline{f'^2}\right) + \frac{\partial}{\partial x_i}\left(\rho u_i \overline{f'^2}\right) = \frac{\partial}{\partial x_i}\left(\frac{\mu_t}{\sigma_t}\frac{\partial \overline{f'^2}}{\partial x_i}\right) + C_g \mu_t \left(\frac{\partial \overline{f}}{\partial x_i}\right)^2 - C_d \rho \frac{\varepsilon}{k}\overline{f'^2} \quad (24)$$

where the constants σ_t, C_g and C_d take the values of 0.7, 2.86, and 2.0, respectively. One advantage of the mixture fraction/PDF model is through the calculation of a single conserved scalar field, f, and other scalars are obtained without solving individual transport equations. In other words, the mixture fraction value at each control volume is used to calculate the instantaneous values of individual species mole fractions, density, and temperature. In an adiabatic system, these instantaneous values depend solely on the instantaneous mixture fraction, f:

$$\varphi_i = \varphi_i(f) \quad (25)$$

where φ_i represents the instantaneous species concentration, density, or temperature. In a non-adiabatic system (e.g., the present study), equation 24 generalizes to:

$$\varphi_i = \varphi_i(f, h^*) \quad (26)$$

where h^* is the instantaneous enthalpy.

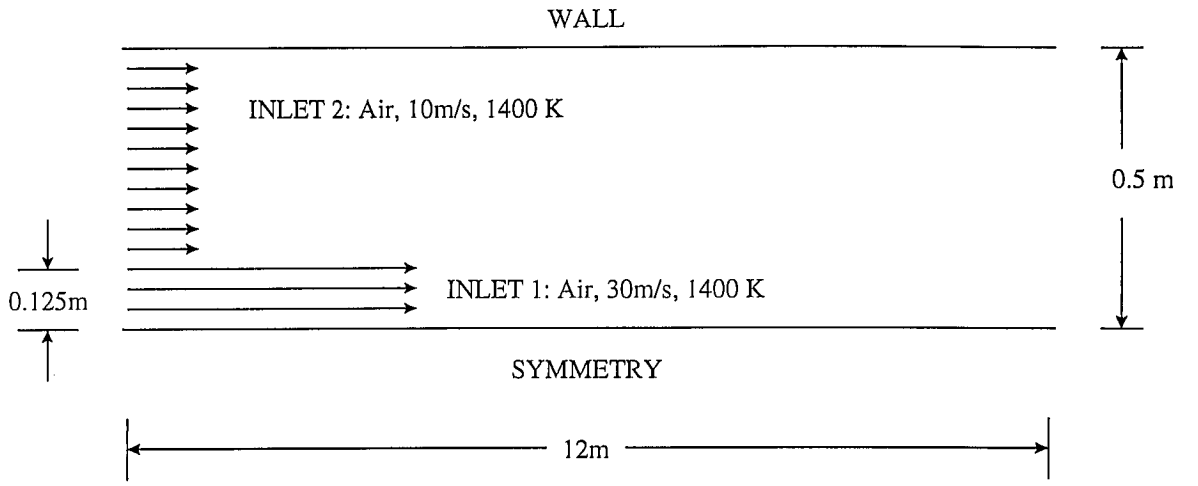

Figure 1: Pulverised Coal Combustion in a Furnace

5. PROBLEM DESCRIPTION

The hypothetical coal combustor considered in this study is a 12m x 1m duct depicted in Figure 1. Due to symmetry only half of the domain width is modelled. The inlet is split into two streams. A high speed stream air flow near the centre of the duct that enters at 30m/s and 1400 K and spans 0.125m. The other stream enters at 10m/s and 1400K and spans 0.375. The wall temperature is taken to be 1100. Coal particles enter the furnace near the centre of the high speed stream with the mass flow rate of 0.05 kg/s. The proximate analysis of a coal studied by Smith et al. (1989), referred to as coal H, is shown in Table 1. The particle size is taken to be 70 μm. The volatile is assumed to be C_3H_8.

Table 1: Chemical Analysis of Coal H (Smith, et. al., 1989)

Air Dried Basis (%W/W)	
Volatile Matter	36.2
Fixed Carbon	51.2
Ash	9.6
Moisture	3.0

6. RESULTS AND DISCUSSIONS

The pulverised coal combustion has been simulated based on the Magnussen and the PDF model. The oxygen concentration in the furnace has been shown in Figures 2 and 3, based on the finite rate chemistry (Magnussen) model and the mixture fraction/PDF approach. Because volatile release occurs slowly in the PDF model results, a significant amount of oxygen is available in the centre of the furnace until relatively far downstream. This occurs because the volatile release (and hence volatile combustion) is relatively slow and oxygen can diffuse into the centre of the furnace more rapidly than it is consumed (Figure 3). This is in contrast to the Magnussen model results in which the oxygen is quite depleted along the centre-line (Figure 2). The availability of oxygen along the furnace centre-line also leads to more complete char combustion in the PDF model results.

The surface reaction rate for char combustion has been shown in Figures 4 and 5 based on the finite rate chemistry (Magnussen) model and the mixture fraction/PDF approach, respectively. In both models the char burnout rate starts almost in the middle of the furnace in which Figures 4 and 5 are magnified to focus on this region. In the Magnussen model, further downstream, the surface reaction is almost negligible near the centre of the furnace despite the presence of Carbon containing coal and the combustion occurs in a short part of the furnace (Figure 4). However, the PDF modelling allows the char burnout to occur in a large part of the furnace (Figure 5). In both models the surface reaction rate decreases because oxygen begins to be depleted as illustrated in Figures 3 and 4.

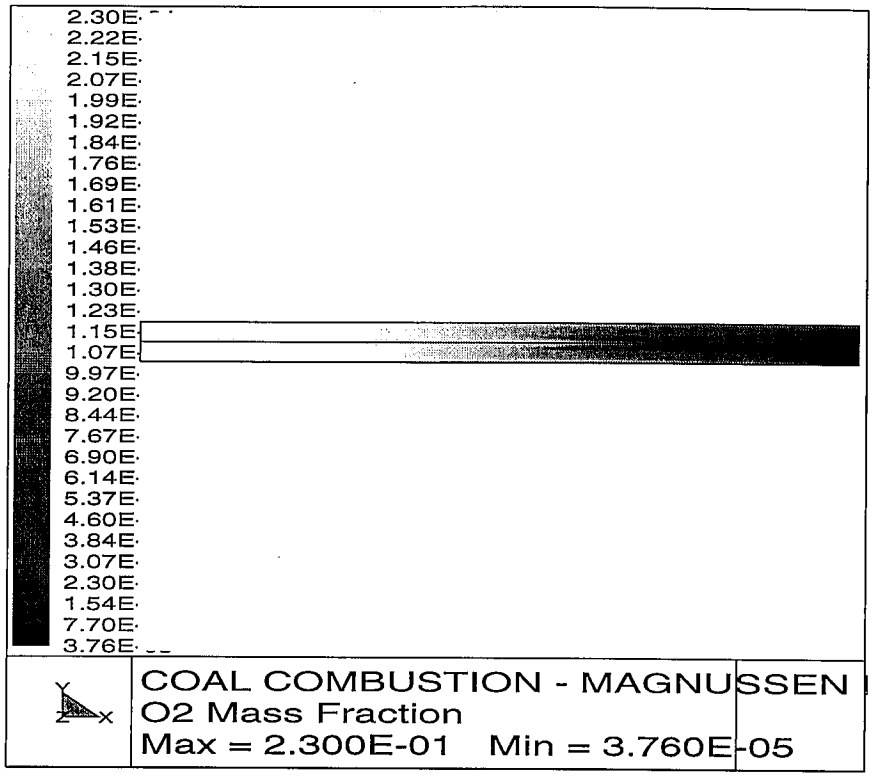

Figure 2: Oxygen concentration, Magnussen Model

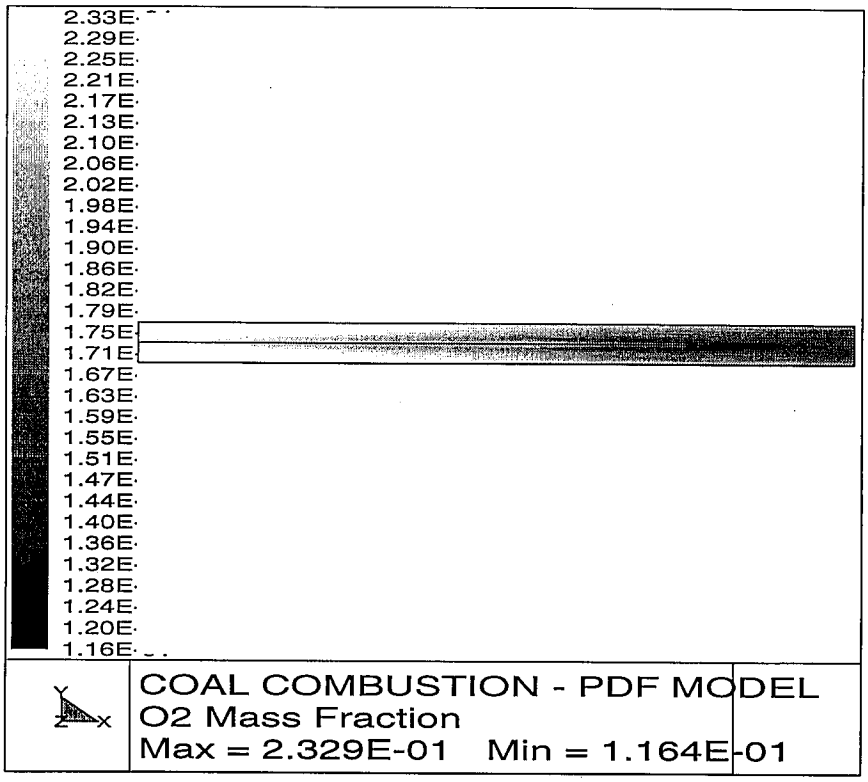

Figure 3: Oxygen concentration, PDF Model

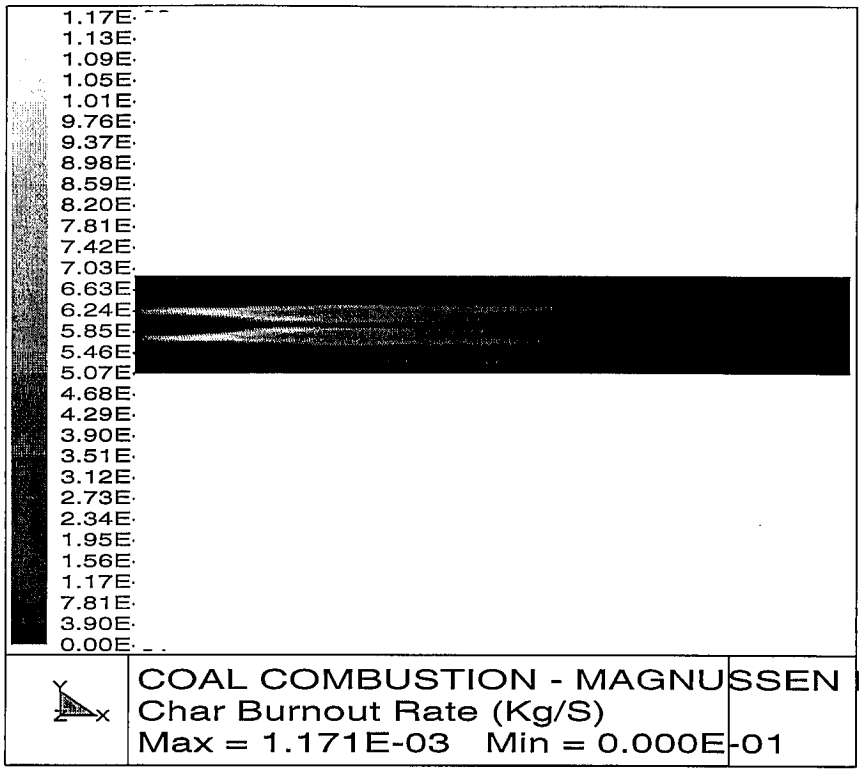

Figure 4: Char burnout rate, Magnussen Model

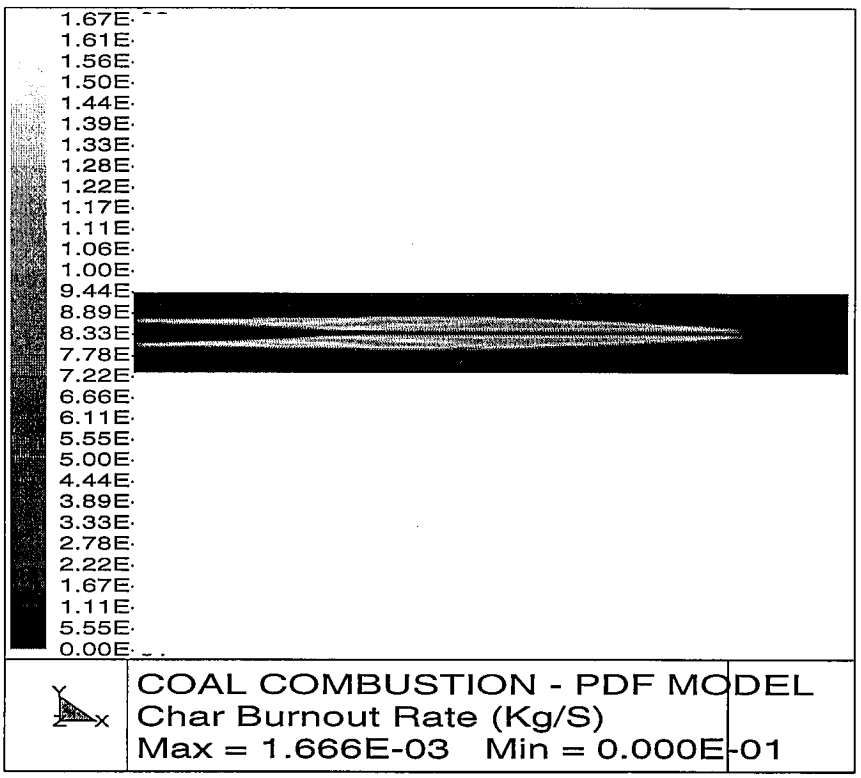

Figure 5: Char burnout rate, PDF Model

7. CONCLUSIONS

A pulverised coal combustion simulation with gas phase flow field and its interaction with a discrete phase of coal particles has been carried out. The devolatilisation of coal particles travelling through gas and char combustion has been simulated. Reaction has been modelled by employing the finite rate chemical kinetics (Magnussen) model and the mixture fraction/PDF method. The mixture fraction/PDF modelling approach, which has been specifically developed for turbulent diffusion flames, offers many benefits over the finite rate formulation. The mixture fraction/PDF model allows intermediate species formation and dissociation effects. It has been demonstrated that the PDF model predicts more realistic results than the Magnussen approach in oxygen concentration and char burnout rate. Since the PDF model does not require the solution of a large number of species transport equations it is computationally efficient.

ACKNOWLEDGEMENTS

The authors wish to acknowledge the support of the CRC for Black Coal Utilisation which is funded in part by the Cooperative Research Centres Program of the Commonwealth Government of Australia.

REFERENCES

Badzioch, S., and Hawksley, P. G. W., 1970, "Kinetics of Thermal Decomposition of Pulverized Coal Particles", *Ind. Eng. Chem.* **9**, 521.

Goerres, J. Schnell, U. And Hein, K.R.G., 1995, "Trajectories of Burning Coal Particles in Highly Swirling Reactive Flows", *Int. Journal of Heat and Fluid Flow*, **16**, pp. 440-450.

Kobayashi, H., Howard, J. B., and Sarofim, A. F., 1976, "Kinetics of Rapid Devolatilization of Pulverized Coal", *16th symp. (Int.) on Comb.,* The combustion Inst., 411.

Magnussen, B.F. and Hjertager, B.H., 1976, "On Mathematical Models of Turbulent Combustion with Special Emphasis on Soot Formation and Combustion", *16th Symp. On Combustion*, Cambridge.

Morsi, S. A. and Alexander A. J., 1972, "An Investigation of Particle Trajectories in Two-Phase Flow Systems", *Journal of Fluid Mechanics*, **55**(2), pp. 193-208.

Sivathann, Y.R. and Faeth, G.M., 1990, "Generalised State Relationships for Scalar Properties in Non-Premixed Hydrocarbon/Air Flames", *Combust. Flame*, **82**, pp. 211-230.

Smith, I.W., Wall, T.F., Baker, J.W., Holcombe, D., Harris, D.J., Juniper, L.A., and, Truelove, J.S., 1989, "The Combustion Behaviour of Low-Volatile Australian Coals", NERDDC Project 1110.

Therssen, E., Gourichon, L. And Delfosse, L., 1995, "Devolatilization of Coal Particles in a Flat Flame", *Combustion and Flame*, **103**, pp. 115-128.